Study of a GBAS model for CAT II/III simulations

Pierre Neri, Christophe Macabiau, Laurent Azoulai

Study of a GBAS Model for CAT II/III Simulations

P. NERI, C. MACABIAU, *ENAC*
L. AZOULAI, *AIRBUS*

BIOGRAPHIES

Pierre NERI graduated as an electronics engineer in 2007 from the ENAC (Ecole Nationale de l'Aviation Civile) in Toulouse, France. Since 2007, he is a Ph.D student at the signal processing lab of ENAC working on multi constellation GNSS receivers for civil aviation.

Christophe MACABIAU graduated as an electronics engineer in 1992 from the ENAC in Toulouse, France. Since 1994, he has been working on the application of satellite navigation techniques to civil aviation. He received his Ph.D in 1997 and has been in charge of the signal processing lab of ENAC since 2000.

Laurent AZOULAI graduated as an engineer specialized in automatic systems in 1996 from ISEP. He has been in charge of development and certification of the first MMR with GBAS Landing System function on Airbus Aircraft. He is working on Approach and Landing functions for Airbus A/C. He is in charge of a function implementing SBAS on A350 XWB and of GBAS Cat II/III airborne project within SESAR. He is also involved in standardization activities dedicated to GBAS Cat 2/3 and GPS/Galileo combination.

ABSTRACT

Since many years, civil aviation has identified GNSS as an attractive mean to provide navigation services for every phase of flight due to its wide coverage area. However, GPS standalone cannot meet ICAO requirements in terms of accuracy, integrity, availability and continuity, particularly in the case of precision approaches. To achieve improved level of performance, different augmentation systems have been developed aiming at enhancing and monitoring the quality of the Signal-In-Space (SIS). In particular, GBAS for Ground Based Augmentation System allows guarantying a very high level of performance in a given coverage area surrounding an airport for example.

Currently, GBAS is foreseen as an important source of innovation for civil aviation since it has already been certified for CAT I precision approaches and may allow reaching ICAO requirements down to CAT II/III minima, then providing an alternative to ILS. This possibility is actively investigated and ICAO and Industry standardization bodies are currently deriving requirements for GBAS CAT II/III.

Autoland simulations for CAT II/III certification require numerous simulations to assess statistically the aircraft capability to autoland. Therefore, it is necessary to identify the GBAS GLS behavior with sufficient fidelity, taking into account physical phenomenon affecting accuracy, continuity and integrity, but still, with adequate limited representativity, assuming that it will feed an autoland simulator dedicated to airworthiness demonstration of aircraft guidance laws.

A model has been proposed in the past but the evolution of CAT II/III requirements and the lack of information on the validation methods used make it necessary to investigate further this subject.

The goal of this paper is to provide the first steps to the development of a model of GBAS L1 C/A depicting the behavior of the outputs of the system with sufficient fidelity for CAT II/III autoland simulations. Our study is based on the previously proposed model. We focused here on the nominal error model which so far appears to be an adequate representation of GBAS behavior for autoland simulations. However, we propose some improvements to update this model so as to reflect the evolution of the requirements and enhance its representativeness while meeting its primary objective to serve airworthiness demonstration. Moreover, additional simulations have been run to extend this model to Cat III airports all over the world since it has been first developed only for North America.

INTRODUCTION

GBAS is very attractive for civil aviation since it allows providing a navigation service with a very high level of performance in comparison with other augmentation systems.

GBAS is composed of a ground station able to compute differential pseudorange corrections and to monitor the quality of the Signal In Space. This station includes several receivers making pseudorange measurements used to process pseudorange corrections and associated integrity data which are sent through a RF data link to the surrounding equipped aircrafts. Using this information, the user receiver is able to correct its own measurements but also to exclude some of them and to compute protection levels which are an evaluation of the confidence that the user can have in the final position solution.

Currently, GBAS has been certified for CAT I precision approaches, and it is anticipated that GBAS can provide further performance to meet CAT II/III requirements. This explains the interest of Civil Aviation, since GBAS may then become an alternative to classical ILS equipments which are currently the only mean to achieve CAT II/III precision approaches. Moreover, ILS equipments are very expensive in terms of installation, qualification, maintenance and needs for flights inspection in comparison with GBAS equipments. This possibility is actively investigated and ICAO and Industry standardization bodies are deriving new requirements for GBAS CAT II/III precision approaches.

The development of these new requirements follows a new concept using GBAS in an innovative fashion. Indeed, this new concept named "GAST D" results from a performance based approach taking credit of aircraft capabilities to allow the use of GBAS technology to reach CAT II/III minima, instead of putting all the constraints on the Signal in Space. In this new approach, there will be a transfer of responsibility from the ground station to the aircraft, unlike ILS. New requirements on the Signal-In-Space and on the airborne side will impact the noise and the errors affecting the outputs of the fault-free on-board receiver which is the interface between GBAS SIS and the autopilot guidance laws. Autoland demonstrations for CAT II/III certification require numerous simulations to assess statistically the aircraft capability to autoland when the autopilot is receiving deviations from an ILS receiver for instance. It is thus necessary to identify precisely the GBAS GLS behavior to perform autoland simulation, in line with applicable regulations for CAT II/III operations.

It is therefore necessary to have a model representing GBAS L1 C/A for autoland simulations purpose. It implies that this model will not be a high fidelity model, but a model adapted to demonstration of autoland capabilities. A model has been published in [Murphy and Harris, 2005] years ago which can model GBAS behavior under nominal, limit and faulted conditions. However, validation methods used have not been described making it necessary to propose new material to provide a consolidated model. Moreover, this model was developed for CAT I simulations, and potentially for CAT II/III simulations, at a time when not all requirements were neither defined nor validated. Since then, CAT II/III requirements have been revised by ICAO and by Industry standards and therefore it is needed to update it to reflect latest developments.

First section is a review of the existing model. It is important to notice that we will focus in the frame of this paper on the nominal conditions model and on the CAT I simulations so as to compare our simulations with the existing results. Then, we present our simulations and the associated results. Finally, some modifications are proposed so as to define the basis of our GBAS L1 C/A noise model.

STATE OF THE ART GBAS NSE MODEL

This model is able to generate GBAS NSE (Navigation System Error) in Nominal condition but also in Limit and Fault case as you can see in Figure 1. However, as stated previously we will focus here on a particular section of the model which is the nominal NSE generator. This module is supposed to generate nominal NSE on the 3 positioning axes which are here along track (atrk), cross track (xtrk) and vertical (vert) directions.

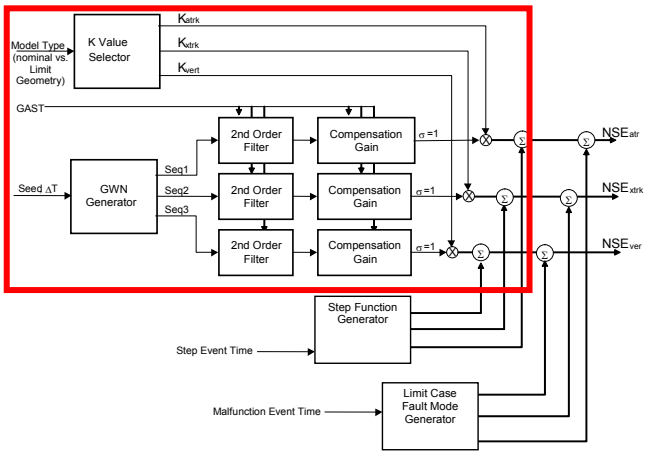

Figure 1 : State of the art GBAS NSE generator [Murphy and Harris, 2005]

To do so, it produces three independent noise sequences with zero mean and unity variance which are filtered by a second-order Butterworth filter, and afterwards normalized. Then, the filter output is scaled by NSE geometry scale factors K_{atrk}, K_{Xtrk}, K_{Vert}. Thus, as we can see here, one particularity of this model is that it does

not model the pseudorange error but it directly generates the error in the position domain.

This approach is interesting since it allows generating only three errors instead of one error for each tracked pseudorange. In the frame of autoland simulations it is a real gain since there are several other parameters that have to be taken into account. However, it is necessary to justify this method.

Projection of pseudorange errors into position domain

The natural relationship between measurement errors and position errors is as follows:

$$dX = \hat{X}(k) - X(k) = A \times E(k) \quad (1)$$

With: $X(k)$ is the aircraft position at epoch k.
$\hat{X}(k)$ is the estimated aircraft position at epoch k.
$E(k) = \begin{bmatrix} e^1(k) \\ \vdots \\ e^n(k) \end{bmatrix}$ is the aggregate of the user pseudorange measurement error including all user possible corrections, plus the GBAS Pseudorange Correction (PRC). It includes residual ionosphere error, residual troposphere error, airborne multipath, air noise, ground multipaths, and ground noise.

- $A = \left[H^t \Sigma^{-1} \mathrm{H}\right]^{-1} H^t \Sigma^{-1}$: This matrix corresponds to the weighted least squares position estimation.
- H is the observation matrix expressed in the local reference frame oriented toward the ideal aircraft trajectory (atrk, xtrk, vert).
- $\Sigma = \begin{bmatrix} \sigma_1^2 & 0 & \cdots & 0 \\ 0 & \sigma_2^2 & \cdots & 0 \\ \vdots & \vdots & \ddots & \vdots \\ 0 & 0 & \cdots & \sigma_n^2 \end{bmatrix}$ where σ_i^2 is the variance of the residual pseudorange error for satellite i. These variances contain all the information on pseudorange errors and that's why it is important to use adequate values.

Thus, the error in the position domain is a linear combination of the pseudorange measurements errors. Let's denote:

$$A(k) = \begin{bmatrix} a_{atrk}^1(k) & \cdots & a_{atrk}^n(k) \\ a_{xtrk}^1(k) & \cdots & a_{xtrk}^n(k) \\ a_{vert}^1(k) & \cdots & a_{vert}^n(k) \\ a_b^1(k) & \cdots & a_b^n(k) \end{bmatrix}$$

Then, we can derive the expression of the different position errors. We begin with the vertical direction:

$$dX_{vert} = a_{vert}^1 . e^1(k) + a_{vert}^2 . e^2(k) + \cdots + a_{vert}^n . e^n(k) \quad (2)$$

We assume that the errors contained in $E(k)$ are modeled as noise processes independent for each satellite. Then, we can represent this positioning error as a single noise process with an adequate variance which is according to eq. (1):

$$\sigma_{vert}^2 = (a_{vert}^1 . \sigma_1)^2 + (a_{vert}^2 . \sigma_2)^2 + \cdots + (a_{vert}^n . \sigma_n)^2$$

$$\sigma_{vert}^2 = \sum_{i=1}^n \left(a_{vert}^i . \sigma_i\right)^2 \quad (3)$$

And then we can write:

$$dX_{vert} = \sigma_{vert} . du_{vert} \quad (4)$$

Where du_{vert} is a process with unity variance resulting from the characteristics of the receiver measurement errors and GBAS corrections. It is the projection of several error components. Thus, time correlation is specific to each of these components. This time correlation has been identified in [Murphy et al., 2009] as the result of the succession of the code tracking loop filter and the code carrier smoothing filter. This will be developed further in the next section.

Therefore, it is equivalent to generate directly the vertical positioning error using the variance σ_{vert}^2 instead of generating each pseudorange measurement error and then projecting it in the position domain.

The same model can be used for the other components of the positioning error:

$$\sigma_{xtrk}^2 = (a_{xtrk}^1 . \sigma_1)^2 + \left(a_{xtr\,k}^2 . \sigma_2\right)^2 + \cdots + (a_{xtrk}^n . \sigma_n)^2 \quad (5)$$

$$\sigma_{atrk}^2 = (a_{atrk}^1 . \sigma_1)^2 + \left(a_{atrk}^2 . \sigma_2\right)^2 + \cdots + (a_{atrk}^n . \sigma_n)^2 \quad (6)$$

And we thus obtain:

$$dX_{xtrk} = \sigma_{xtrk} . du_{xtrk} \quad (7)$$

$$dX_{atrk} = \sigma_{atrk} . du_{atrk} \quad (8)$$

The processes du_{vert}, du_{xtrk}, du_{atrk} are correlated in time individually and with each other and moreover σ_{vert}, σ_{xtrk}, σ_{atrk} are not independent.

This statistical model for the GBAS position error conforms to the model proposed in [Murphy and Harris, 2005]. Then, our model and the state of the art model will be based on the same statistical base.

We can deduce from our developments that the *K* factors used in the GBAS NSE generator correspond exactly to the standard deviations we have highlighted:

$$K_{vert} = \sigma_{vert}, K_{xtrk} = \sigma_{xtrk}, K_{atrk} = \sigma_{atrk} \quad (9)$$

In fact, weighted least squares theory tells us that to compute these standard deviations we can use a more direct method. We know that the covariance matrix C of the position estimation error is given by:

$$C = (H^T \Sigma^{-1} \mathrm{H})^{-1} \quad (10)$$

Therefore, we have simply:

$$\begin{cases} {\sigma_{atrk}}^2 = C(1,1) \\ {\sigma_{xtrk}}^2 = C(2,2) \\ {\sigma_{vert}}^2 = C(3,3) \end{cases} \quad (11)$$

Where $C(i,j)$ is the coefficient of matrix C in row i and column j.

Now, the idea is to generate the three processes du_{vert}, du_{xtrk}, du_{atrk}.

2nd order filter reproducing time correlation

The solution used in [Murphy and Harris, 2005] is to generate three independent white Gaussian noise sequences with zero mean and unity variance. Each noise sequence is then filtered by a second-order Butterworth filter whose transfer function can be written as in [Murphy and Harris, 2005]:

$$H(s) = \frac{\omega_n^2}{s^2 + \sqrt{2}\omega_n . s + \omega_n^2} \quad (12)$$

Where $\omega_n = 0.01\, rad/sec$

This filter is justified in [Murphy et al., 2009]. Assuming that the error entering a GBAS receiver is white Gaussian, then the spectral content of the error on the smoothed pseudorange measurements is determined by two processes:

- The code tracking loop (DLL) filtering
- The carrier smoothing

What is important for us is that the carrier smoothing uses a 100 seconds time constant.

With the development of new requirements for CAT II/III it will be necessary to include a different time constant for this filter, which will be 30 seconds. Also, we will review the justification for the introduction of this filter.

A compensation gain is then used to scale the standard deviation of the outputs of the filter to unity. This compensation gain is simply obtained by computing the standard deviation of the filter outputs.
When obtaining these processes, the most important elements are the K values since it will drive the standard deviations of the processes and so the shape of the final errors.

Vertical NSE magnitude: Kvert

The NSE scale factors Kvert, Kxtrk, Katrk are used to control the standard deviation of NSE errors in the vertical, cross-track and along-track directions. These quantities are driven by pseudorange measurement errors and satellite geometry. In the model, they are obtained by sampling a value x from a uniform distribution between 0 and 1. Then, Kvert is obtained using the following expression in the case of GAST C:

$$K_{vert} = \mathrm{f(x)} = 0.4 + 0.2\mathrm{x} - \frac{0.004}{\mathrm{x}-1} \quad (13)$$

This function was determined by simulating satellite geometry from different airport locations. Then, assuming that the position solution is a weighted least squares solution, it is possible to compute the covariance matrix which contains the variance of the errors of estimation of the position. These simulations are detailed in [Murphy et al., 2009]. What is important to notice is that these simulations were conducted only for LAAS (Local Area Augmentation System) coverage area and so it may be interesting to verify if these results are applicable to other locations.

This final expression of Kvert gives a bound to the maximum values of sigma_vert observed during simulations presented in [Murphy et al., 2009] over seven different airports.

Horizontal NSE magnitudes: Kxtrk and Katrk

In the case of horizontal NSE error magnitudes, it was decided to consider the worst cross-track error possible. In fact, depending on aircraft trajectory, the horizontal error is distributed differently between cross-track and along-track components. This assumption therefore implies to choose the runway heading producing the largest cross-track error.

As for Kvert, several simulations were conducted to compute the covariance matrix under this assumption. Nonetheless, instead of studying directly σ_{xtrk}, they decided to watch the ratio between σ_{xtrk} and σ_{vert}. The goal was to determine a unique ratio between σ_{vert} and σ_{xtrk}. In fact, one can see that it would allow generating only Kvert and deducing Kxtrk from it instead of generating two different values from two different distributions.

With the results obtained, they highlighted a particular point: $\sigma_{xtrk}/\sigma_{vert} = 0.818$. Therefore defining:

$$K_{xtrk} = 0.818 \times K_{vert} \quad (14)$$

They evaluated that the probability that the cross-track NSE error magnitude computed using this method exceed

the actual one was about 2.10^{-5}. This choice was considered as conservative and has been implemented in the model.

They also decided to set the along-track component variance to the same value as the cross-track component:

$$K_{xtrk} = K_{atrk} = 0.818 \times K_{vert} \quad (15)$$

With this method the number of variables of the model is clearly reduced.

Now that we have presented the state of the art model we will detail the simulations that have been run so as to evaluate its validity.

GBAS NSE MODEL SIMULATIONS: VERTICAL NSE MAGNITUDE

Simulation assumptions for Kvert determination

To determine the distribution of the coefficient Kvert we have computed the covariance matrix associated to the weighted least squares estimation of position in several locations and under some assumptions which are listed below.

We used the standard 24 satellites GPS constellations and we considered all possible constellations states with up to two satellites removed from service. We could have taken into account more satellite failures but we had to limit this parameter because of time constraints. Therefore, we had to use the probabilities of satellite failures that are gathered in Table 1. As we can see, there are two different sets of probabilities. In fact, the first set corresponds to the probabilities used in [Murphy et al., 2009]. Indeed, these appeared to be very conservative to us. It was published in [RTCA,1997]. These probabilities have been updated in [RTCA, 2004] to provide more realistic values. This second set f probabilities is far less conservative. We decided that for comparison purpose we would use the same probabilities as in [Murphy et al., 2009] during initial simulations, but for all our final results we used the more appropriate ones found in [RTCA, 2004]. As we considered only two maximum satellite failures at the same time we decided to overestimate the probability of 22 operational satellites:

$$P(22\ operational\ satellites) = 1 - 0.95 - 0.03 = 0.02 \quad (16)$$

Computations were made each second over a 24 hours period and at different locations. We considered the same locations as in [Murphy et al., 2009] but we also added new airports so as to generalize the results. The list of airports is given in Table 2 with the associated coordinates. We also added what we called high latitudes locations to illustrate the evolution of the results for latitudes from 70° to 85°.

Number of Operational Satellites N	Probability of N operational satellites used in [Murphy et al., 2009]	Probability of N operational satellites DO-245A [RTCA, 2004]
24	0.72	0.95
23	0.17	0.03
22	0.064	0.012
21	0.026	0.0048
20	0.02	$0.03 \times 0.34^{(23-N)}$

Table 1 : Constellation states probabilities

Location	Latitude (°)	Longitude (°)	Altitude (m)
Anchorage	64.174361	-149.996361	46.33
Dallas	32.896828	-97.037996	185.01
New York City	40.639751	-73.778926	3.96
Los Angeles	33.942522	-118.407161	38.10
Miami	25.793250	-80.290556	2.44
Chicago	41.978143	-87.905870	204.83
Seattle	47.4498889	-122.311778	132.00
Johannesburg	26.148175	28.134939	20.00
Dakar	14.738436	-17.488747	20.00
Brussels	50.901702	4.483025	20.00
Hong Kong	22.316478	113.936553	20.00
Sydney	-33.933078	151.177550	20.00
Tokyo	35.769655	140.389686	20.00
Beijing	39.960555	116.256944	20.00
Lat 0 airport	0.000000	-122.311778	20.00

Table 2 : Simulation Locations

Finally we had to decide what would be the performance of the GBAS ground station and of the airborne receiver. We chose to use DO-245A designations and thus, we considered GAD (Ground Accuracy Designator) = B3, AAD (Airborne Accuracy Designator) = A and AMD (Airframe Multipath Designator) = A. If we refer to [RTCA, 2004] it leads to the following expressions for variance of pseudorange measurements:

$$\sigma_i^2 = \sigma_{pr\_gnd,i}^2 + \sigma_{pr\_air,i}^2 + \sigma_{mp,i}^2 \quad (17)$$

With: σ_i^2 variance of the i[th] pseudorange measurement

$$\sigma_{pr\_gnd,i} \leq \sqrt{\frac{\left(0.16 + 1.07 e^{-\theta_i/15.5}\right)^2}{3} + (0.08)^2} \quad (18)$$

$$\sigma_{pr_{air},i} \leq 0.15 + 0.43 e^{-\theta_i/6.9} \quad (19)$$

$$\sigma_{mp,i} \leq 0.13 + 0.53e^{-\theta_i/10.0} \quad (20)$$

θ_i the elevation of the satellite in degrees

Our approach is different here from the previous methods since these expressions were not available at the time. Moreover, as we can see, we only consider bounds to the true variances and then we may be conservative. However, these expressions are standardized and therefore we prefer to use it. In [Murphy et al., 2009] different expressions were used which were supposed to model a nominal error and not a bound. These expressions are the following [Murphy et al., 2009]:

$$\sigma^2_{pr\_gnd,i} = \underbrace{\frac{\left(0.16+1.07e^{-\frac{\theta_i}{15.5}}\right)^2}{2} + 0.08^2}_{GAD=B2} + \underbrace{\left(\frac{0.03}{\sin(\theta_i)}\right)^2}_{Residual\ Iono\ and\ Tropo} \quad (21)$$

$$\sigma^2_{pr\_air,i} = \underbrace{\left(0.11 + 0.13e^{-\frac{\theta_i}{4}}\right)^2}_{AAD=B} + \underbrace{\left(0.2e^{-\frac{\theta_i}{75}}\right)^2}_{MultipatHs} \quad (22)$$

We have identified the different contributions in the formulas. Some weaknesses have been identified in these expressions and in particular the multipaths model which is known for underestimating the multipaths error.

Using the model of these variances, we want to determine statistics of Kvert, Kxtrk and Katrk.

When the pseudorange measurement errors are defined, one difficulty is to deal with the different constellation states.
We recall the expressions found for the variances of GBAS NSE:

$$\begin{cases} {\sigma_{atrk}}^2 = C(1,1) \\ {\sigma_{xtrk}}^2 = C(2,2) \\ {\sigma_{vert}}^2 = C(3,3) \end{cases} \quad (11)$$

With: $C = (H^T \Sigma^{-1} \mathrm{H})^{-1}$ (10)

If we consider each constellation states then we will obtain for example 23 different values when considering one satellite failures out of 24 satellites. We have then to combine properly these values. Here is our model.

If we denote Y the positioning error in the vertical direction then:
${\sigma_{vert}}^2 = E[Y^2]$ (23)
We consider two additional random variables $X1$ and $X2$ representing the number of satellite failures and the id of the faulted satellites. Note that the number of satellites failures and the id of the faulted satellites are not the only random variables to consider. We also take into account the visible satellite constellation and the position as random. However, here we consider a simplified problem to ease the understanding. Then we can write:
$E[Y^2/X1] = E_{X2}\left[E[Y^2/(X1,X2)]\right]$ (24)

This means that to obtain the ${\sigma_{vert}}^2$ value considering for example 23 operational satellites we just have to compute the mean of the 23 ${\sigma_{vert,23}}^2$ values computed corresponding to the 23 possible constellation states since it are equiprobable.

We can apply the same idea to obtain the final ${\sigma_{vert}}^2$:

$${\sigma_{vert}}^2 = E[Y^2] = E_{X1}[E[Y^2/X1]]$$

$${\sigma_{vert}}^2 = E[Y^2] = P(24\ op\ sat).{\sigma_{vert,24}}^2 + P(23\ op\ sat).{\sigma_{vert,24}}^2 + P(22\ op\ sat).{\sigma_{vert,22}}^2 \quad (25)$$

We have finally obtained Kvert which is the square root of ${\sigma_{vert}}^2$. We have to notice that we also decided to reject all values of σ_{vert} that would exceed the value of 1.736m which corresponds to a Vertical Protection Level (VPL) larger than the Vertical Alert Limit (VAL) of 10 meters because in this case the system would be declared unavailable which is not under our scope at the moment. We have to note that in the new GBAS Cat III concept currently developed by ICAO, the VAL used by the aircraft will be lower than 10 m, according to geometry screening process and associated thresholds, leading to exclude more values of ${\sigma_{vert}}^2$.

Kvert simulation results for airports locations (latitude<70°)

On the basis of our simulations we computed different histograms and Cumulative Density Functions (CDF) which are shown below and compared to some of the results presented in [Murphy et al., 2009].

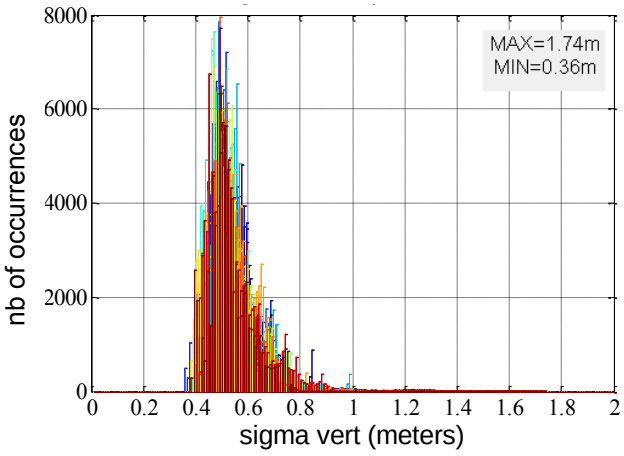

Figure 2 : σ_{vert} histogram superimposed for all airports using same probabilities as in [Murphy et al., 2009]

We can see by comparing figure 3 and 4 that our results are slightly higher than the ones in [Murphy et al., 2009]. This can be more easily seen in the following figures.

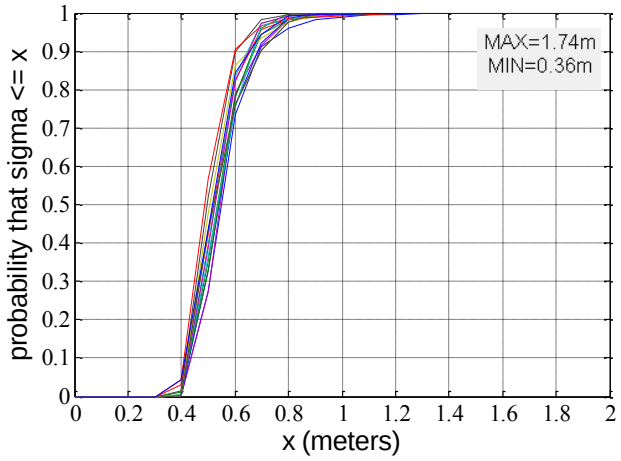

Figure 3 : σ_{vert} CDF for all airports using same probabilities as in [Murphy et al., 2009]

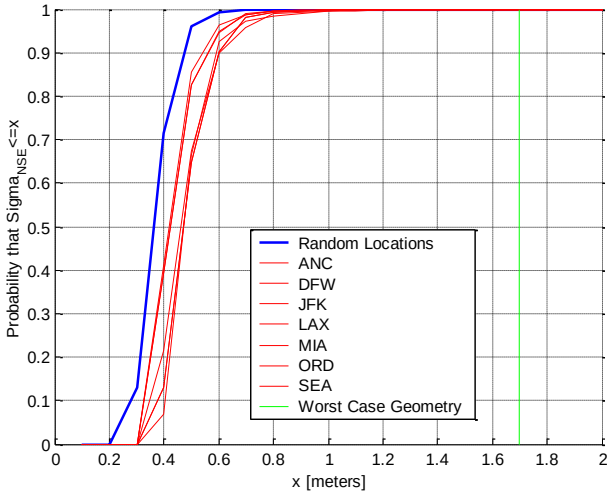

Figure 4 : σ_{vert} CDF for all airports published in [Murphy et al., 2009]

In Figure 5, we plotted the CDF inversing the axes just as it was done in [Murphy et al., 2009] to determine the K value generation function (See eq. 13). We can clearly conclude here that the sigmas are higher than state of the art ones since it exceeds the function used to generate Kvert and which was supposed to be a bound. This must be due to the fact that we did not use exactly the same sigmas as in [Murphy et al., 2009] for characterizing pseudorange measurement errors. In fact, we used overbounds of the sigmas which may have led us to over estimating the error. However, we used a more appropriate multipath model which we knew would inflate the results.

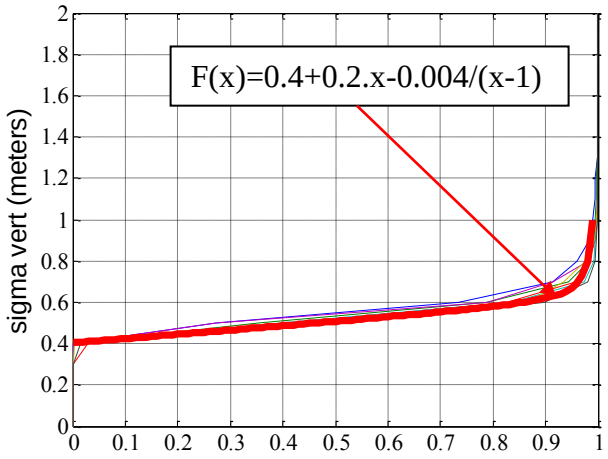

Figure 5 : comparison between computed CDF and function to generate K values proposed in [Murphy et al., 2009]

Our next step was to observe the impact of different constellation states probabilities. Until now, we used the ones from [Murphy et al., 2009] presented in first column of Table 1. We will now present results obtained using the second column containing DO-245A values.

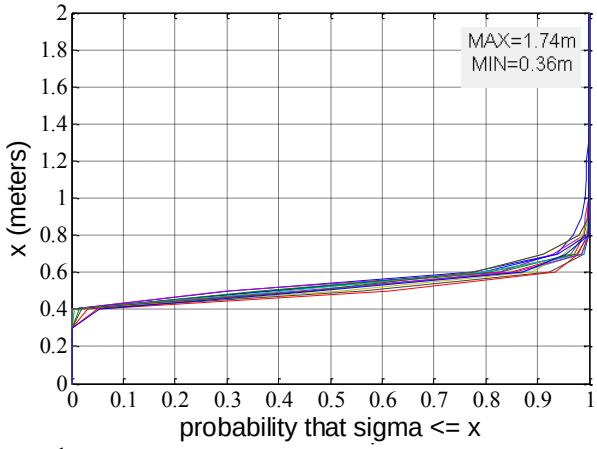

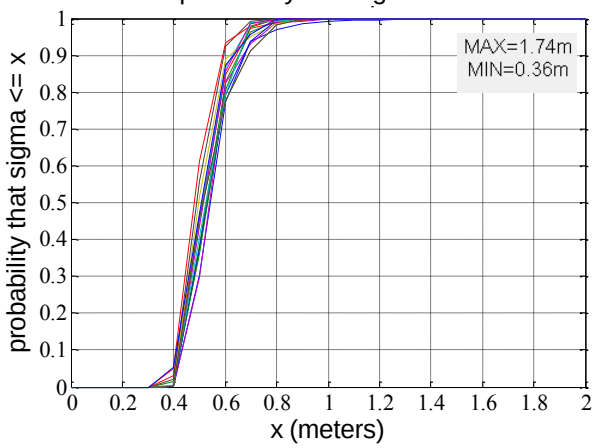

Figure 6 and 7 : σ_{vert} CDF for all airports using DO-245A probabilities

Only small differences can be noticed by comparing Figure 6 to figure 3. We can observe a little difference between Figure 2 and Figure 8. We can see that high values of $\sigma_{vert}{}^2$ are more rarely observed. This is easily understandable, since with the new set of probabilities we increased the contribution of full constellation operational which should provide the best results in terms of precision. To conclude, the difference brought by the set of probabilities from DO-245A is not so obvious but since DO-245A probabilities seem more realistic, we decided to use it as reference for the rest of our simulations.

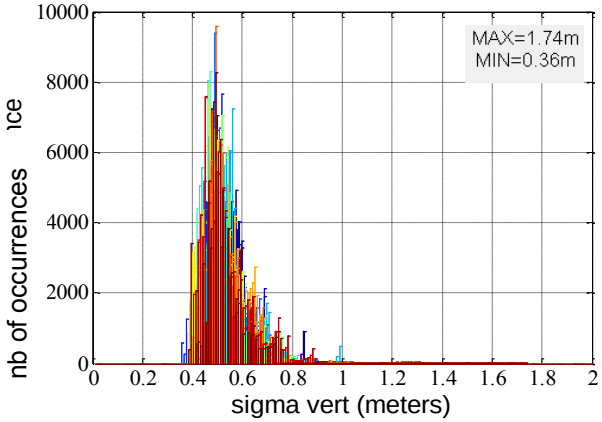

Figure 8 : σ_{vert} histograms superimposed for all airports using DO-245A probabilities

Kvert simulation results for high latitudes (|lat|>=70°)

During our simulations we noted that for high latitudes, results are quite different from what we have seen until now. That's why we dedicated a section to high latitude cases and we tried to illustrate the evolution of the vertical NSE magnitude with the latitude.

We can see the results in Figure 9 and Figure 10. As expected the accuracy is degrading when getting closer to the pole due to the bad geometry. For specific airports, it may then be useful to build a model linked to the latitude when passing 70° of latitude. This could be studied in a future step of these activities.

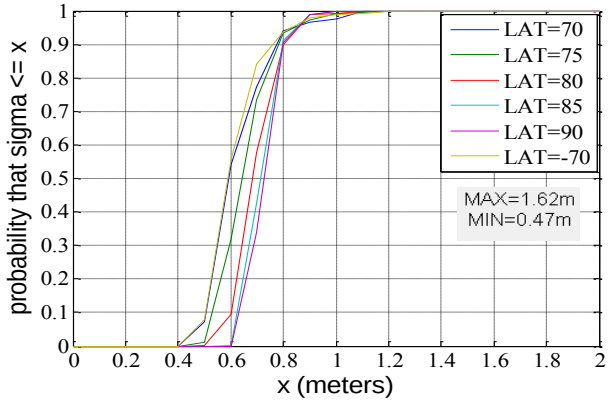

Figure 9 : σ_{vert} CDF for high latitudes

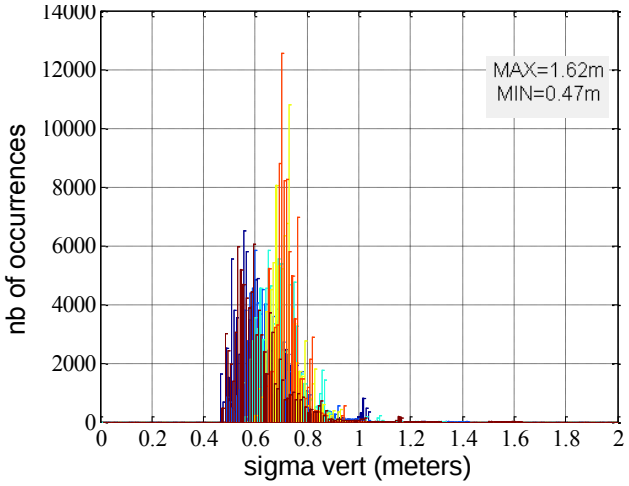

Figure 10 : σ_{vert} histograms superimposed for high latitudes

GBAS NSE MODEL SIMULATIONS: HORIZONTAL NSE MAGNITUDE

Simulation assumptions for Kxtrk and Katrk determination

It seems that two different simulations have been realized in [Murphy et al., 2009] to compute Horizontal and Vertical NSE magnitude. Instead, we computed all values at the same time because we were able to compute the whole covariance matrix of the positioning error. Thus, the simulations assumptions are the same as for Vertical NSE magnitude determination.

However, one difficulty is to use the following assumption: we considered the runway heading producing the largest cross-track error. Therefore, we had to determine this particular direction. Knowing that the distribution of the error is ellipsoidal in the horizontal plane, our goal was to determine the major axis and minor axis of the corresponding ellipse. This can be done by diagonalizing the Covariance matrix C. For clarity purpose we will focus on the horizontal part of the matrix C that we call C_{horr} :

$$C_{horr} = \begin{bmatrix} C_x(1,1) & C_x(1,2) \\ C_x(2,1) & C_x(2,2) \end{bmatrix} \quad (26)$$

We then computed the eigen vectors and eigen values of this matrix:

$$\text{Eigenvectors: } V_1 = \begin{bmatrix} \cos(\theta) \\ \sin(\theta) \end{bmatrix} \text{ and } V_2 = \begin{bmatrix} -\sin(\theta) \\ \cos(\theta) \end{bmatrix} \quad (27)$$

$$R = [V_1 \quad V_2]$$

Eigenvalues: λ_{maj} , λ_{min}

With θ the rotation angle between the north, east reference frame (which was used as the basis coordinate frame) and the obtained reference frame.
The eigenvalues exactly correspond to minor and major axis of the ellipse and using the eigenvectors we were able to determine the runway heading producing these maximum errors.

Kxtrk, Katrk simulation results for airports locations (latitude<70°)

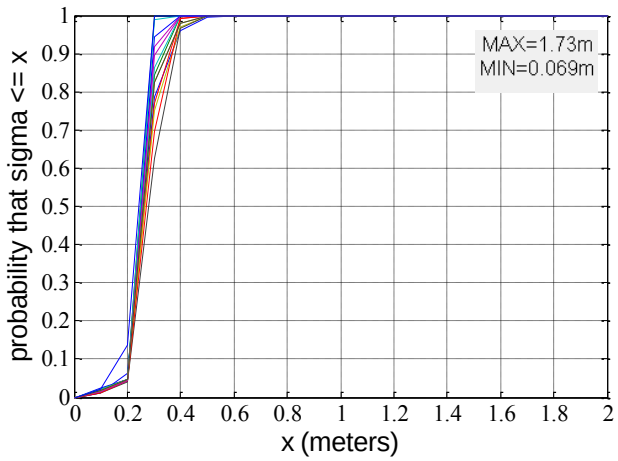

Figure 11 : σ_{xtrk} CDF for all airports

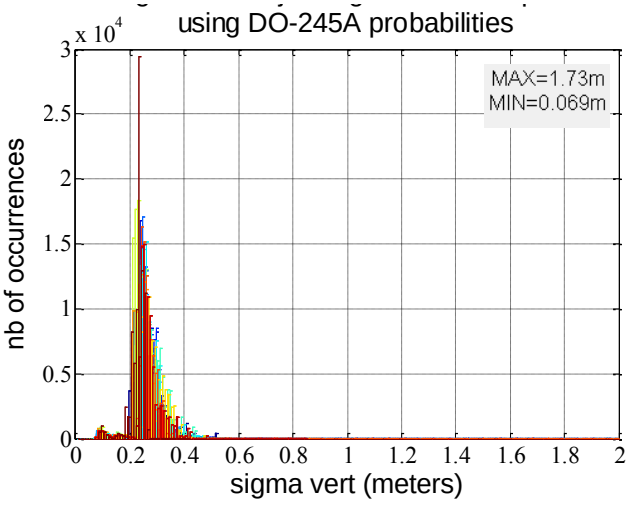

Figure 12 : σ_{xtrk} histograms superimposed for all airports

In Figure 11, Figure 12, Figure 13 and Figure 14 we present the results obtained for σ_{xtrk} and σ_{atrk}. As we can see, vertical error is bigger than horizontal as we could expect. Horizontal errors are globally very small except for some cases that can be explained by bad geometries mainly.

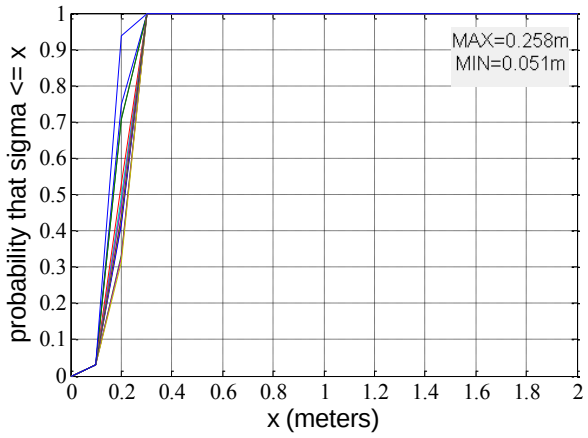

Figure 13 : σ_{atrk} CDF for all airports

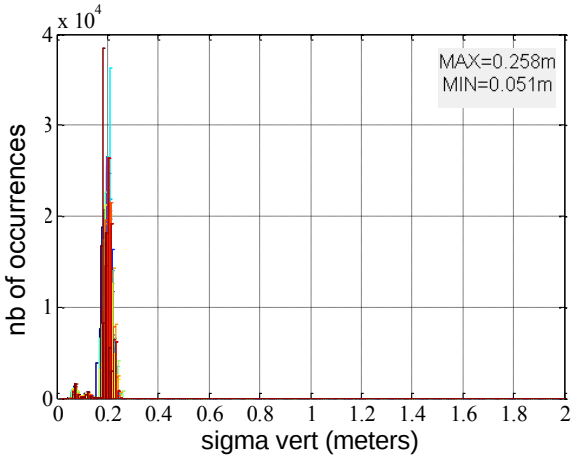

Figure 14 : σ_{atrk} histograms superimposed for all airports

Ratio between horizontal and vertical components

As stated in equation (15), the state of the art GBAS NSE model uses a constant ratio to deduce horizontal NSE magnitudes from vertical NSE magnitude. We computed the ratio that we could observe using our results. The final results can be observed in Figure 15 and Figure 16. We can see, in Figure 15 that the ratio chosen in [Murphy et al., 2005] and represented by the red horizontal line is rarely exceeded. According to our simulations the probability that the ratio $\sigma_{xtrk}/\sigma_{vert}$ exceeds the value 0.818 is equal to about 4.10^{-4}. It has to be compared with the probability announced of 2.10^{-5}. This can be explained by two facts. First, we added other locations to our simulations which may have introduced new geometries. Second, we did not use the same expressions for standard deviations of pseudorange measurements errors. However, the scale factor is still quite good and can then be used. Still, we will propose a different way of generating horizontal scale factors at the end of this paper.

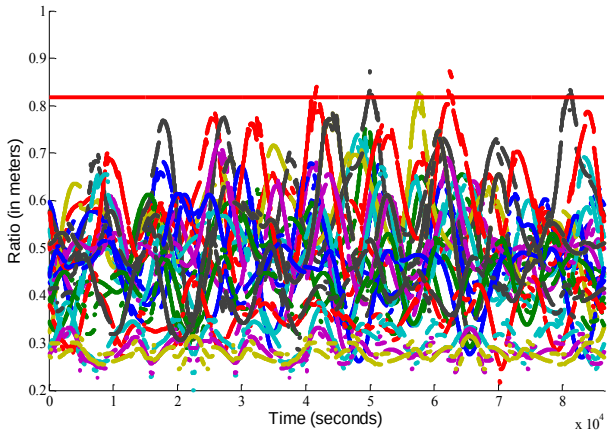

Figure 15 : $\sigma_{xtrk}/\sigma_{vert}$ for all airports during 24 hours simulation

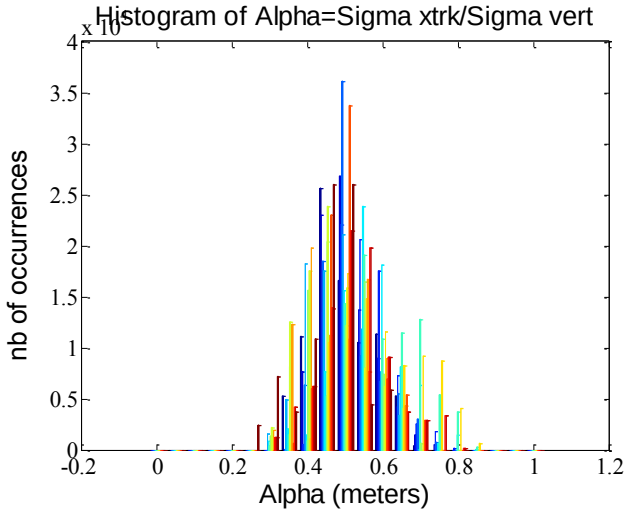

Figure 16 : $\sigma_{xtrk}/\sigma_{vert}$ histogram superimposed for all airports

Correlation between vertical and horizontal NSE

It is stated in [Murphy et al., 2009] that tests have been run to check if it was necessary to implement a correlation algorithm to account for satellites geometry correlation with time. Their conclusion was that no additional correlation was necessary since the second-order Butterworth filter was introducing sufficient correlation. This is due to the 100 s smoothing filter. Since we have obtained new results we decided to make the same verification.

To do so, we first had to compute the correlation coefficient between vertical and horizontal errors. This was a formality since we already computed the covariance matrix C of the positioning error which gives the cross-correlation between vertical and cross-track errors. Thus, the correlation coefficient is given by:

$$\rho_{vert\,/xtrk} = \frac{\sigma_{vert\,/xtrk}}{\sigma_{vert}\,.\sigma_{xtrk}} \tag{28}$$

We obtained the distribution presented in Figure 17. This distribution is not the same as the one presented in [Murphy et al., 2009]. That's why it is interesting to check the necessity of an additional correlation algorithm.

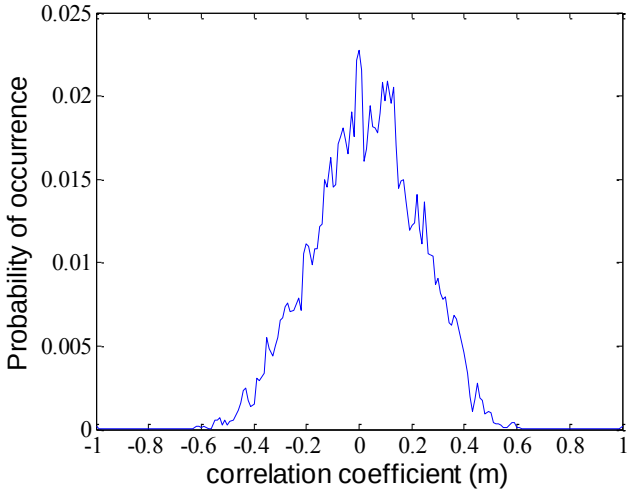

Figure 17 : Correlation Coefficient between vertical and xtrk errors

To do so we made the following experiment. We repeated 2000 times the generation of two series of 360 seconds white noise sequences. Each sequence was then filtered by the 2nd order filter (eq. 12). We then computed the correlation coefficient of the two filtered sequences. This was the first part of the test. The second one was to apply a correlation algorithm given in [Murphy et al., 2009] so as to introduce additional correlation using the previous distribution as input. We remind the correlation algorithm:

$$\begin{bmatrix} N_1 \\ N_2 \end{bmatrix} = \begin{bmatrix} 1 & 0 \\ \rho & \sqrt{1-\rho^2} \end{bmatrix} \begin{bmatrix} S_1 \\ S_2 \end{bmatrix} \tag{29}$$

Where: S_1 and S_2 are the filtered sequences
N_1 and N_2 are the filtered and geometrically correlated sequences
ρ is the desired correlation coefficient

The results are presented in Figure 18 and 19. What we can see here is that as expected, the correlation algorithm has no major effects on the correlation between the two sequences. Obviously, the 2nd order filter representing tracking loops and smoothing filter creates a correlation which is not altered by the geometrical correlation.

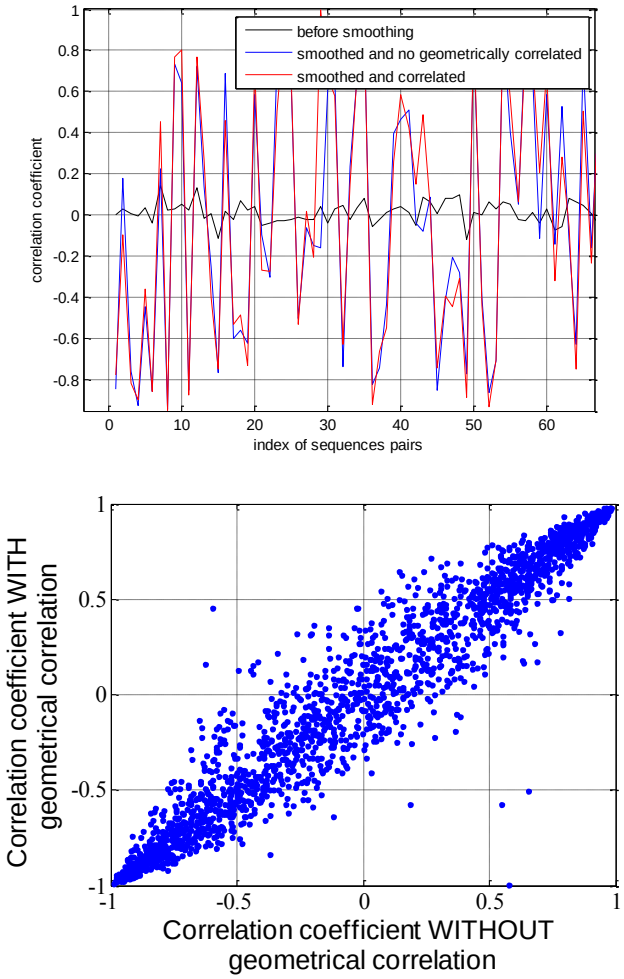

Figure 18 and 19 : Comparison of correlation coefficient before and after geometrical correlation

PROPOSED MODIFICATIONS OF GBAS NSE MODEL

We have already presented different modifications of the simulation assumptions that we have implemented:

- Standard deviation of pseudorange measurements errors have been modeled differently.
- Probabilities of satellite constellation states have been updated with more realistic quantities.

These parameters concern the preliminary simulations to determine K factors distributions. The following statements concern more the principle of the model and more particularly the K factors generation.

For the nominal vertical NSE model, instead of creating a function to generate Kvert, our approach would be to memorize its histogram. To obtain it we sum and normalize the histograms obtained for all airports. We obtain the result presented in Figure 20.

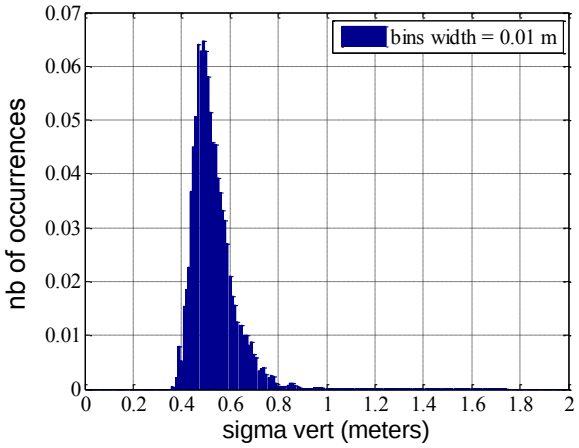

Figure 20 : σ_{vert} histogram

Then we would draw Kvert directly from σ_{vert} distribution so as to reflect our observations.

For the nominal horizontal NSE model, the state of the art model uses a worst case constant scale factor to generate cross-track error. This may be too much conservative since our goal is to model the nominal behavior of GBAS NSE error. That's why we propose to generate Kxtrk by drawing it from σ_{xtrk} observed distribution which is shown in Figure 21, just as for Kvert.

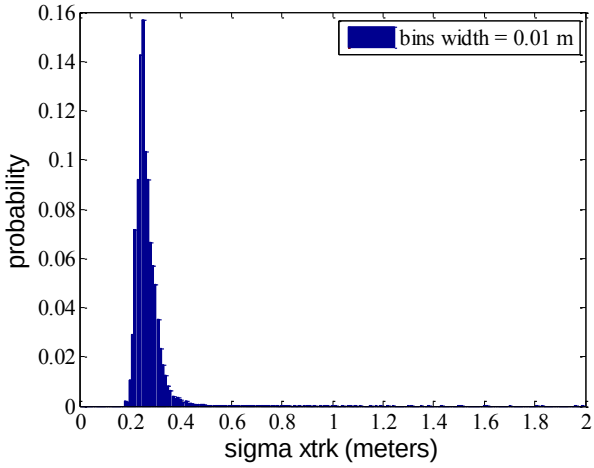

Figure 21 : σ_{xtrk} histogram

With these values and the associated bins, it is possible to randomly select a value from these histograms and therefore, approximate the distributions of σ_{xtrk} and σ_{vert}. This method presents two advantages. The first one is that using a histogram for σ_{vert} allows not computing an approximate function such as the one used in the state-of-the-art model which is taking infinite values when getting close to unity (See eq. 13). The second one is that by modeling directly σ_{xtrk} using its own histogram we

will not always compute the worst horizontal NSE magnitude and we will model several different σ_{xtrk} / σ_{vert} ratios. However, our proposal is not perfect since the drawback of this method is that we suppose that σ_{xtrk} and σ_{vert} are independent which is not true. In fact, the risk is that we may observe more often high values of σ_{xtrk} and at the same time low values of σ_{vert}. This case would happen with a probability of 10^{-2}. Therefore, we believe that it will be necessary to define a mechanism to control the number of occurrence of this situation. Finally, we think that assuming that Kxtrk is equal to Katrk is a good assumption even if it is conservative.

CONCLUSIONS AND WAY FORWARD

The state of the art analysis has shown that a GBAS NSE model for autoland performance simulations has already been developed [Murphy et al., 2009]. This model assumes that the GBAS NSE can be modeled as three independent sequences scaled by sigmas factors drawn from experimental distributions. Our model will be based on the same model. The state of the art model then assumes a 2nd order filter representing tracking loops and code-carrier smoothing, and scaled by sigmas factors drawn from experimental distributions. The horizontal sigmas factors are 0.818 times the vertical sigma.

However, the lack of information on the validation methods used has led us to investigate the validity of this model. Also, some aspects of this model need to be updated to take into account recent GBAS standards for CAT II/III.

Our work first focused on observations of the vertical NSE magnitude with our software over airports of interest for us. Taking into account the new standard pseudorange error sigmas and our airports the sigma distribution that we observe is larger than the sigma distribution proposed in the state of the art model. We also propose here to distinguish between airports with latitudes > 70° and other airports.

Concerning the horizontal sigma distribution, based on our analysis and observations with our software, we propose to draw a separate horizontal sigma to reflect the diversity between vertical and horizontal sigmas, with a limiting technique to prevent observing too frequent large horizontal to vertical sigmas ratio. The cross-track and along-track are chosen identical. No privileged runway heading appears in our simulation in average on earth.

This work was the first part of our study. Our results will be completed with the analysis of the second order filter and of the two other modules of the state of the art GBAS NSE model which are the step function generator and the fault mode generator. The first one account for steps due to constellation changes and the second one account for fault conditions. Finally, a model will be proposed to update the state of the art model.

REFERENCES

[RTCA, 1997]: LAAS MASPS Draft 06, *Minimum Aviation System Performance for Local Area Augmentation System*, RTCA, 1997.

[Murphy and Harris, 2005]: Document D683447-5 *Characterization of the GBAS System Output*, W. M. Harris, T. A. Murphy, 2005.

[Murphy et al., 2009]: *SARPS Support for Airworthiness Assessments GLS Signal modeling*, T. A. Murphy, 2009.

[RTCA, 2004]: DO-245A *Minimum Aviation System Performance Standards for Local Area Augmentation System*, RTCA, 2004